KFKI
8/1969

ION OPTICS OF A HOMOGENEOUS ACCELERATOR TUBE WITH QUADRATIC ENTRANCE

L. Varga

HUNGARIAN ACADEMY OF SCIENCES
CENTRAL RESEARCH INSTITUTE FOR PHYSICS

BUDAPEST

ION OPTICS OF A HOMOGENEOUS ACCELERATOR TUBE WITH QUADRATIC ENTRANCE

L. Varga
Central Research Institute for Physics, Budapest, Hungary

Abstract

A method is described for improving the ion optical properties of a homogeneous accelerator tube by appropriately modifying its entrance aperture. It is shown that a low magnification can be ensured by simple means without pre-acceleration.

1. Introduction

The essential investigations on the ion optics of homogeneous accelerator tubes had been made by M. Elkind[1] more than ten years ago. Ever since that time his work has underlain the design concepts for tubes of this type. In the years past considerable progress was made in improving the calculation methods[2] as well as in developing new matching sections between the ion source and the tube[3,4], to compensate the thousand times difference between the energies of particles exiting from the soruce and the tube. The matching has to meet some mechanical, electrical and optical requirements such as accuracy, high breaking strength, low aberrations, low magnification, regulability, and, if possible, self-focusing. The simultaneous satisfaction of these requirements but difficult, and most of such systems have room for improvement. At present the system developed by Johnson et al[3] seems to be the best, for this system however, high-level technical means, and tubes with low loading are needed. Owing to the rapid increase in magnification in terms of the energy multiplication of the accelerator, observable for all of the currently used three-element tubes[1], preacceleration is inevitably needed. Keeping the over-all energy multiplication unaltered, the net magnification can be remarkably decreased by modifying the axial field distribution by using the combination of an immersion lens, and a three-element tube instead of a simple three-element tube.

The axial field of the electrostatic generator[5], type EG-2 of our Institute has been modified to enable us to operate the source and the accelerator without any preacceleration. The optical parameters of an accelerator tube depend mainly on the aperture at its entrance, thus, investigations were made on the variations in optical properties with modifications in the initial E_1-E_2 transition. Sufficiently low magnification is obtainable by adequate modification of the axial field-distribution even for a few thousand times energy multiplication, and the ion source can be mounted directly at the upper tube end, without any matching element between them.

2. Quadratic optics

Although the running - up of field strenght is ad libitum variable, in the present paper a quadratic initial potential distribution is considered. This is convenient for design and an exact solution of the paraxial ray equation can be obtained. In the interest of generality in the initial E_1-E_2 transition $E_2 \neq 0$, thus not a three- but a four - element tube is discussed /Fig.1/, where the elements are as follows:

1/ Aperture with transition from $E_1 = 0$ to $E_2 \neq 0$

2/ Quadratic section with potential distribution

$$U(z) = U_0 + E_2 z + \frac{E_3 - E_2}{2l} z^2 \qquad /1/$$

where "l" is the quadratic section lenght.

3/ Homogeneous section with field strenght E_3.

4/ Aperture at the lower tube-end with transition from $E_3 \neq 0$ to $E_4 = 0$.

The following is to present the transition matrices of the four elements.

2.1 The optical paramters of the first aperture were obtained in the same way as in 1/, however, in the interest of higher accuracy, f in 1/ was completed by a term involving the aperture deameter instead of the factor ξ. The D/f value calculated by numerical integration in ref.[6], can be well approximated by

$$\frac{D}{f} = \frac{1}{4}\left[D\,\frac{E_2 - E_1}{U_0} - \left(\frac{D}{3{,}1}\cdot\frac{E_2 - E_1}{U_0}\right)^{1{,}4}\right] \qquad /2/$$

the formula being used instead of $\frac{D}{f} = \frac{D}{4} \cdot \frac{E_2 - E_1}{U_0}$ in ref.[1].
For $0 < \frac{D(E_2 - E_1)}{U_0} < 20$ the results show only a few percent error relative to the D/f values obtained by numerical integration and presented in ref.[6]. Assuming the principal planes of the aperture lens to coincide in the aperture plane, the transition matrix* can be given, as

$$[\alpha] = \begin{pmatrix} 1 & 0 \\ -\frac{1}{4}\left[\frac{E_2}{U_0} - \frac{D^{0,4}}{5}\left(\frac{E_2}{U_0}\right)^{1,4}\right] & 1 \end{pmatrix} \qquad /3/$$

2.2 Quadratic section. Replaicing $\frac{dx}{dz}$ with $[U(z)]^{-1/2}$ the paraxial ray equation takes the form

$$\ddot{r} + U\frac{r}{4} = 0 \qquad /4/$$

where the dots and prines denote differentiations with respect to x and z, respectively. Substituting Eq /1/ into Eq. /4/, the differential form, describing the trajectory in the second optical element, is

$$\ddot{r} + \frac{E_3 - E_2}{4l} \cdot r = 0 \qquad /4a/$$

The solution of Eq. /4a/ is

$$r(z) = r_0 \cos\theta(z) + r_0' \cdot 2\sqrt{\frac{U_0}{U''}} \cdot \sin\theta(z)$$

$$r'(z) = -\frac{r_0}{2}\sqrt{\frac{U''}{U_{(z)}}} \cdot \sin\theta(z) + r_0'\sqrt{\frac{U_0}{U_{(z)}}} \cdot \cos\theta(z) \qquad /5/$$

where $\theta(z) = \frac{1}{\sqrt{2}} \ln \frac{U'(z) + \sqrt{2U(z) \cdot U''}}{U_0 + \sqrt{2U_0 + U''}}$

---

* The transition matrix is determined by $\begin{pmatrix} r \\ r' \end{pmatrix} = [\alpha] \cdot \begin{pmatrix} r_0 \\ r_0' \end{pmatrix}$, where r_0 and r are the radial distances of the trajectories of the beginning and the end of an optical element, respectively, and r_0, r' are their slopes at theese places.

let be $\frac{E_2}{E_3} = \varepsilon$; $\frac{l}{K} = \lambda$; $\frac{r}{K} = \rho$ and $\frac{U_0 + U_{acc}}{U_0} = N$ /6/

The trajectory parameters at $z = l$ can be determined from those at $z = 0$ by the matrix:

$$[\beta] = \begin{pmatrix} \cos\theta(\lambda) & \lambda\sqrt{2}\sqrt{\frac{\varepsilon+1+2/\lambda}{(1-\varepsilon)(N-1)}}\cdot\sin\theta(\lambda) \\ -\frac{\sin\theta(\lambda)}{\lambda\sqrt{2}}\cdot\sqrt{\frac{1-\varepsilon}{1+\varepsilon+\frac{\varepsilon-1+2/\lambda}{N-1}}} & \frac{\cos\theta(\lambda)}{\sqrt{1+\frac{(1+\varepsilon)(N-1)}{\varepsilon-1+2/\lambda}}} \end{pmatrix} \quad /7/$$

Now $$\theta(\lambda) = \frac{1}{\sqrt{2}}\ln\frac{1+\sqrt{(1-\varepsilon)^2+(1-\varepsilon)\frac{\varepsilon-1+2/\lambda}{N-1}}}{\varepsilon+\sqrt{(1-\varepsilon)\frac{\varepsilon-1+2/\lambda}{N-1}}}$$

2.3 The particle exiting the quadratic section is passed to the homogeneous section with E_3 field. From the linear relationship between parameters r_0, r_0' and r, r' at the beginning and end of this section, respectively, the transition matrix has the form

$$[\gamma] = \begin{pmatrix} 1 & \lambda\left(1+\varepsilon+\frac{\varepsilon-1+2/\lambda}{N-1}\right)\left(-1+\sqrt{1+2\frac{1/\lambda-1}{1+\varepsilon+\frac{\varepsilon-1+2/\lambda}{N-1}}}\right) \\ 0 & \left(1+2\frac{1/\lambda-1}{1+\varepsilon+\frac{\varepsilon-1+2/\lambda}{N-1}}\right)^{1/2} \end{pmatrix} \quad /8/$$

where the symbols are the same as before.

2.4 On passing through the output the beam enters the field $E_4 = 0$. This transition is considered corresponding to 1/.

The fourth matrix

$$[\delta] = \begin{pmatrix} 1 & 0 \\ \frac{1}{2\lambda N}\cdot\frac{N-1}{\varepsilon-1+2/\lambda} & 1 \end{pmatrix} \quad /9/$$

where the symbols are kept unaltered.

2.5 The product of the four matrices equals the matrix [O] of the whole optical system, where the elements O_{ij} are

$$O_{11} = \beta_{11} + \gamma_{12}\beta_{21} + (\beta_{12} + \gamma_{12}\beta_{22})\alpha_{21}$$

$$O_{12} = \beta_{12} + \gamma_{12}\beta_{22}$$

$$O_{21} = \delta_{21}O_{12} + \gamma_{22}(\beta_{21} + \beta_{22}\alpha_{21}) \qquad /10/$$

$$O_{22} = \delta_{21}O_{12} + \gamma_{22}\beta_{22}$$

respectively.

The elements of matrix [O] determined numerically for various N, λ and $\mathcal{E}$ values are tabulated in the Appendix. The results hold for a given value of D/K, namely 7.10^{-3}. The assignment of a given value to D/K, does not introduce essential restrictions to generality since the parameters bear only loosely upon D/K. D/K occurs in the O_{11} and O_{21} elements through the α_{21} matrix element only. Making numerical test it can be stated that decreasing D/K form 7.10^{-3} to $1{,}4.10^{-3}$ /i.e. by a factor of 5/ the increase in O_{11} and O_{21} is only 5 per cent for N=1000, $\mathcal{E} = 0{,}2$ and $\lambda = 0{,}1o5$. In the case of decreasing $\mathcal{E}$'s, the effect produced by D/K is smaller since for small $\mathcal{E}$'s the quadratic section is dominant as compared with the aperture.

On completing the optical system with two field-free sections /Fig. 1/ preceding and succeeding it /s = σ.K and p=q.K since the object and image distances measured in tube-lenght units are σ and q, respectively/ the matrix [Ω] consists of elements

$$\omega_{11} = O_{11} + qO_{21} \qquad \omega_{12} = \sigma O_{11} + O_{12} + q(\sigma O_{21} + O_{22})$$

$$\omega_{21} = O_{21} \qquad \omega_{22} = \sigma O_{21} + O_{22} \qquad /11/$$

If the 'object' vector is at a distance σ.K before the accelerator tube τ, t' /the particle trajectory is at distance t = τ.K from the axis and has a slope t'/, then in p = qK the particle passes through the 'image' plane at

$$K = \frac{k}{K} = \tau(O_{11} + qO_{21}) + t[\sigma O_{11} + O_{12} + q(\sigma O_{21} + O_{22})]$$

with slope

/12/

$$k' = \tau O_{21} + t'(\sigma O_{21} + O_{22})$$

2.6 Although these results are enough to predict points X, k' associated with given points τ, t', the determination of beam diameter, and the methods for minimizing it, are of much more practical importance. Let /12/ be written in the form

$$t' = -\tau \frac{O_{11} + qO_{21}}{\sigma O_{11} + O_{12} + q(\sigma O_{21} + O_{22})} + K \frac{1}{\sigma O_{11} + O_{12} + q(\sigma O_{21} + O_{22})} \quad /13/$$

Evidently, all of the poinsts τ, t', that lie within the emittance--diagram /holding at a distance σK from the tube entrance/ on the straight line defined by

$$t'_{\tau=0} = \frac{X}{\sigma O_{11} + O_{12} + q(\sigma O_{21} + O_{22})}$$

and

$$\psi = -\frac{O_{11} + qO_{21}}{\sigma O_{11} + O_{12} + q(\sigma O_{21} + O_{22})} \quad /14/$$

are transformed into the same X /Fig.2/. If this line has no common point with the emittance-diagram, at X cannot be a point of any particle trajectory. The marginal points X_1 and X_2 of the beam in a plane-of-observation /at distance qK from the tube-end/ can be determined by framing the diagram with two straight lines tangential to it at τ_1, t'_1 and τ_2, t'_2, the slope $\psi(\sigma, [O], q)$ of which for given values of σ and $[O]$, depends on q.

Let the function $\psi(\sigma, [O], q)$ be analysed with respect to its q-dependence. For given values of σ and [O] it can be seen that

a/ both its numerator and denominator has a zero point, i.e.

$\psi = 0$ if $\quad q = -\frac{O_{11}}{O_{21}} = q_0$

and /15/

$$\psi = \infty \quad \text{if} \quad q = -\frac{O_{11}}{O_{21}} \cdot \frac{\sigma + O_{12}/O_{21}}{\sigma + O_{22}/O_{21}} = q_\infty$$

---

* Note: In geometrical optics - O_{11}/O_{21} determines the second focal point, while $-O_{22}/O_{21}$ the first one of the optical systeme [O]

b/ if $q \longrightarrow \pm \infty$, then $\Psi \longrightarrow \Psi_\infty = \frac{1}{\sigma + O_{22}/O_{21}}$ i.e.
$\Psi_\infty \lessgtr 0$ if $\sigma + \frac{O_{22}}{O_{21}} \lessgtr 0$

c/ $\left.\frac{\partial \Psi}{\partial q}\right|_{q=q_0} = \frac{Det[O]}{O_{21}^2}$ i.e. its first derivative is positive.

d/ $\left.\frac{\partial^2 \Psi}{\partial q^2}\right|_{q=q_0} = 2\frac{\sigma + O_{22}/O_{21}}{(O_{12}/O_{21} - \frac{O_{11}O_{22}}{O_{21}})^2}$ i.e. the sign of the second derivative is the same as that of $\sigma + O_{22}/O_{21}$.

The sign of $\sigma + O_{22}/O_{21}$ depends on that the 'object' point is before or behind the 'focal' point /15a/. These two versions are shown in Fig. 3. Although q_0 can be either positive or negative, its practical values for the optical system under investigation were found to be less than zero. /See in Appendix./ From /12/ we have

$$\chi(q_\infty) = \tau \frac{Det[O]}{O_{21}(\sigma + O_{22}/O_{21})} \qquad /16/$$

indicating that any trajectory passing through χ/q_∞ / has the same initial coordinate τ at σ, independently of its individual slope. Since $O_{21} < 0$,/see in Appendix/ the signs of χ/q_∞ / and can be either identical or different depending on that the σ lies before or behind the 'focal' point.

$\chi/q_0/$ can be determined by the equation

$$\chi(q_0) = -t\frac{Det[O]}{O_{21}} \qquad /17/$$

where the sign of $\chi/q_0/$ is the same as that of t'.

From the Appendix and /17/. it can be seen that $\chi/q_0/$ continuously dicreases with increasing energy multiplication /at least for N's up to the order of 10^3/. Using the results obtained from analyzing the q-dependence of Ψ, the beam diameter can be determined provided the emittance-diagram is known. In ref,[7] an ion source is described which has been designed for use with the accelerator complete with the ion optical system described here. The emittance diagram of this source /see the dotted line in Fig.4/ can be transformed into a form framable by two straight lines parallel to the axis t', and simplify the treatment let the diagram be completed to a rectangular /see the solid line in Fig.4/ by two straight lines parallel to the axis τ. This can be done without introducing any significant error. Assuming this corrected diagram to present the beam's cross-section at σ, its two parallel tangents, determine the points τ, t' of the particle trajectories

whose intersections with the plane-of-observation at q are the marginal points of the beam's cross-section in that plane.

Besides the above stright lines with slope $\Psi\,/q_o/=0$ and $\Psi\,/q_\infty/=\infty$ any other line with slope $-\infty<\Psi(q)<+\infty$ can be tangential to the rectangle but at its corners $\pm\,\tau_m$, $\pm\,t'$, only. As shown in Fig. 3, the marginal points in a plane at distance $q_\infty<q<q_o$ from the tube-end correspond to points $+\,\tau_m$; $+\,t'_m$ and $-\,\tau_m$; $-t'_m$ of the emittance-diagram in Fig. 4 if $/\,\sigma_o + O_{22}/O_{21} < 0$, while for any other q's the initial parameters $-\,\tau_m$; $+t'_m$ or $+\,\tau_m$; $-t'_m$. If $q_o<q<q_\infty$, the marginal trajectories are started from points $-\,\tau_m$; $+t'_m$ and $+\,\tau_m$; $-t'_m$, while for q's outside this interval the trajectories started from the other two corners are marginal. Evidently, the marginal trajectories are the same in each case, in the first one without, in the second with cross-over within the interval q_o-to-q_∞. Variations in the beam diameter for q's within the interval q_o-to-q_∞ were found to be less that those for q's outside of it.

The q-dependence of the beam diameter for given [O] and various σ's has been so far considered. It is however, of much more pratical importance to adjust the N in an optical system with given emittance, σ_o, ε and λ to give minimum diameter at $q = q_T > 0$. Although for a given [O] and σ_o, $q_\infty([O],\ \sigma_o) \neq q_T$, there must be another $\sigma_1 \neq \sigma_o$ where $q_\infty([O],\ \sigma_1) = q_T$.

If the form of diagram shown in Fig. 4 corresponds to the emittance at σ_o, then its form transformed with respect to the distance $\pm\,(\sigma_1-\sigma_o)$ corresponds to that at σ_1. Here $t'_m(\sigma_o) = t'_m(\sigma_1)$, and $|\tau_m(\sigma_1)| = |\tau_m(\sigma_o)| + |t'_m(\sigma_1-\sigma_o)|$. /See the $\tau_m(\sigma)$ of Fig.5/. Since now $q_T = q_\infty$, the coefficient of t' in /12/, equals zero, thus

$$\chi(q_\infty) - \chi(q_T) = (O_{11} + q_\infty O_{21})\cdot\tau(\sigma_1) = M\cdot\tau(\sigma_1) \qquad /18/$$

i.e. $\chi\,/q_T/$ is the product of $\tau_m/\,\sigma_1\,/$ and the magnification factor: M. σ and the magnification M are shown for various values of λ and N in Fig.5. where $q_T = 1$, and $\varepsilon = 0$, and a schematic plot of the function $\tau_m/\,\sigma\,/$ is also shown. Evidently, the shape of the function $\tau\,/q,\,\sigma\,/$, thereby of $\chi\,/q_T,N/$ depends primarily on $\tau_m/\,\sigma\,/$ if $M/\,\sigma\,/$. It is about constant /e.g. for λ=0,15; 0,2; 0,5/, while for a rapidly varying $M/\,\sigma\,/$ /e.g. λ=0; see Ref. 1/ the function $\chi\,/q_T,N/$ cannot be minimum at σ_o.

For special parameters of emittance it may thus occur that the minimum spot diameter at q_T is obtained for a value of N other than that required to image the minimum cross-section of the source's output beam onto the target.

The dependence of the optical system under investigation on the parameters is numerically illustrated also in Fig. 6 where $q = 1$ and N is constant.

Mounting the source directly on the upper tube end, N, ε , and λ can be choosen to result in a magnification low enough to permit a sufficiently small spot even for a considerably wide range of high-voltage.

2.7 Making use of the focusing procedure described in 2.6 investigations were made on the broadening of the beam diameter during acceleration. In a three-element tube the beam diameter is the greatest at the entrance, however in our case a significant broadening in the quadratic section has to be considered. Evidently, the maximum diameter must be within the interval λ since exiting from there the beam is subject to no more focusing within the tube. "r" in /5/ is a periodic function of z and may have extreme value /or values/ at Z_m determined from r'/z/=0 by solving

$$tg\Theta(z_m) = 2\,\frac{r_o'}{r_o}\sqrt{\frac{U_o}{U''}}$$

Making use of the previous symbols, and assuming [O] to image the cross-ower at σ_o.K into q_T.K; whereafter the object is considered as a point, whith $r_o' = \frac{\rho_T}{\sigma_o}$ we have

$$tg\Theta(z_m) = \frac{\lambda\sqrt{2}}{\sigma_o}\sqrt{\frac{\varepsilon-1+2/\lambda}{(N-1)(1-\varepsilon)}} \qquad /19/$$

and from /7/

$$\frac{\rho(z_m)}{\rho_o} = \frac{r(z_m)}{r_o} = \cos\Theta(z_m)\left[1+\frac{\lambda\sqrt{2}}{\sigma_o}\sqrt{\frac{\varepsilon-1+2/\lambda}{(N-1)(1-\varepsilon)}}\,tg\,\Theta(z_m)\right] =$$

$$= \left[1+tg^2\Theta(z_m)\right]\cos\Theta(z_m) \qquad /20/$$

The maximum broadening of beam relative to its entrance diameter for given values of λ and ε can be calculated by /20/. r_o depends on N through $\sigma_o.K$, since in the case of various N's the point-source emitting with maximum slope r'_{on} must be mounted at various $\sigma'_o.K$ distances from the tube. Using $r_o = \sigma_o.Kr'_{om}$ we have $r/Z_m/=r'_{om}K.f/N/$

$$f(N) = \sigma_o\left[1+tg^2\Theta(z_m)\right]\cos\Theta(z_m) \qquad /21/$$

On the basis of data in the Appendix f/N/ was calculated also numerically for q = 1 and various associated values of λ and ε. The results are shown in Fig.7. One can see that over the most important range of λ and ε the curves almost cover each other, and for the practical values of N, f/N/ is rather small, offering the advantage that the beam emitted by the source with a great divergence can be accelerated in a tube with $D > 2r\ (z_m)$.

3. Field distribution

The axial potential distribution corresponds to /1/ if

$$U(r,z) = U_o + E_2 z + \frac{E_3 - E_2}{2l}\cdot\left|z - \frac{r^2}{2}\right| \qquad /22/$$

Present form of U/r,z/ satisfies the Laplace-equation.

3.1 Let the electrodes be spaced by d along the axis z /Fig.8/. Obviously, the elecrrodes must be convex in direction -z, such that the centre of the one mounted at $z = n.d$ should be at distance $\xi.d$ above the electrode plane. Let the electrode shape fit the equipotential passing through the point $r = 0$, $z = d/n - \xi$ / and cross the plane $z = nd$ at the $r = d.\sqrt{2}$ /Fig.8/.

Although $r = d\sqrt{2}$ was chosen at will to simplify the numerical evaluation, this value is necessary and seems to be enough to eliminate the effect produced by geometrical error /the electrode deteriorates to a plane, in the subsection ' $r > d.\sqrt{2}$/.

Corresponding to these premisses we have

$$U[r=0;\ z=d(n-\xi_n)] = U(r=d\sqrt{2};\ z=nd)$$

wherefrom ξ_n can be determined by /22/, as

$$\xi = \left(\frac{\varepsilon}{1-\varepsilon}\cdot\frac{l}{d}+n\right) - \sqrt{\left(\frac{\varepsilon}{1-\varepsilon}\cdot\frac{l}{d}+n\right)^2 - 1} \qquad /23/$$

where the symbols are as before, and to eliminate $\xi_n > 1$ the square root has expressively negative sign. Making use of the expression

$$\nu = \frac{\varepsilon}{1-\varepsilon}\cdot\frac{l}{d}+n$$

the function $\xi(\nu)$ is presented in Fig. 9. l/d shows the number of steps of the increase from the field εE_3 to E_3. From Fig. 9 it can be seen, at what distance is the centre of the n-th electrode above the plane r at z = n.d, for given ε and l/d values. One can see that for $\nu \geq 6$–8 the order of magnitude of electrode thickness is almost reached, thus the shaping to convex form is not necessary.

For smaller ν values a spherical surface is the most advantageous to approximate the ideal equipotential. The radius of curvature for the spherical surface passing through the circle of $r = d.\sqrt{2}$ radius, drawn through points $z = /n - \xi_n/.d$ and $z = n.d$ can be determined from the expression

$$R = d\left[\nu + \frac{1}{2\xi(\nu)}\right]$$

which tends to $2d.\nu$ for $\nu \geq 2$. This approximation is good enough even for $\nu = 2$ /the error is about 3 per cent/. Care must be taken in the case of $\varepsilon = 0$ and $n = 1$. Now $\xi = 1$, hence $z - 0$, and the spherical surface is definable but a better approximation can be obtained by direct considerations with the use of /22/. Owing to $\varepsilon = 0$ becomes

$$tg\,\varphi = \frac{r}{z} = \sqrt{2}$$

i.e. the first electrode has to be a cone with opening of $2\varphi = 109^{\circ}28'$ and with its peak at the point z = 0.

3.2 There must be determined the divider supplying the operational voltage for the geometry discussed above. Comparing the potential difference between the n-th and /n-1/ th electrodes with that between the $n = (l/d-1)$ - th and $n = l/d$-th ones/ the last and the last but one electrode in the quadratic section/ and assuming a constant divider current, the resistances in the divider will be obtained relative to the last resistor's value.

The relative resistances to be used in the n-th section can be determined from

$$\frac{R_n}{R_{max}} = \frac{\Delta U(n)}{\Delta U(\frac{1}{d}-1)} = \frac{2\varepsilon\frac{1}{d}+(1-\varepsilon)(2n-1)}{2\frac{1}{d}-(1-\varepsilon)} \qquad /24/$$

Evidently the values are linearly increasing.

Notes

It is a question, whether the loading affects the voltage set by the divider. In our opinion the loading affects the end face rather than the accelerator electrodes. From the linear increase in field strenght it follows that the initial section of the accelerator tube can not be entirely utilized for energy multiplication, although the loss of lenght $\frac{\lambda(1-\varepsilon)}{2}$ is acceptably small /about 5 per cent in practice/. As regards the breaking strength, it is advantageous that the loading is relatively small at the tube entrance where the collimated, fast neutral beam originating from the source has not yet been distributed.

Acknowledgments

Thanks are due to Miss E. Haviár for her help in numerical evaluations as well as to Mr. L. Királyhidi for the tank tests concerning the solution of problems in field distribution.

Appendix

$\lambda = 0$ $\varepsilon = 1$

N	O_{11}	O_{12}	O_{21}	O_{22}
80	-2.351	$2.011\ 10^{-1}$	-2.443	$1.614\ 10^{-1}$
160	-3.620	$1.465\ 10^{-1}$	-3.392	$1.154\ 10^{-1}$
320	-5.137	$1.058\ 10^{-1}$	-4.520	$8.229\ 10^{-2}$
640	-6.764	$7.605\ 10^{-2}$	-5.724	$5.851\ 10^{-2}$
1280	-8.102	$5.438\ 10^{-2}$	-6.702	$4.153\ 10^{-2}$
2560	-8.195	$3.875\ 10^{-2}$	-6.737	$2.945\ 10^{-2}$

$\lambda = 0{,}05$ $\varepsilon = 0$

N	O_{11}	O_{12}	O_{21}	O_{22}
80	-1.916	$1.582\ 10^{-1}$	-2.121	$1.168\ 10^{-1}$
160	-2.597	$9.594\ 10^{-2}$	-2.593	$6.536\ 10^{-2}$
320	-3.179	$5.180\ 10^{-2}$	-2.960	$3.066\ 10^{-2}$
640	-3.597	$2.265\ 10^{-2}$	-3.176	$9.017\ 10^{-3}$
1280	-3.811	$4.974\ 10^{-3}$	-3.211	$-3.141\ 10^{-3}$
2560	-3.800	$-4.592\ 10^{-3}$	-3.058	$-8.895\ 10^{-3}$

$\lambda = 0{,}05$ $\varepsilon = 0.1$

N	O_{11}	O_{12}	O_{21}	O_{22}
80	-1.863	$1.656\ 10^{-1}$	-2.070	$1.240\ 10^{-1}$
160	-2.523	$1.060\ 10^{-1}$	-2.523	$7.474\ 10^{-1}$
320	-3.096	$6.416\ 10^{-2}$	-2.883	$4.169\ 10^{-2}$
640	-3.536	$3.648\ 10^{-2}$	-3.114	$2.095\ 10^{-2}$
1280	-3.818	$1.927\ 10^{-2}$	-3.203	$8.850\ 10^{-3}$
2560	-3.938	$9.229\ 10^{-3}$	-3.152	$2.369\ 10^{-3}$

$\lambda = 0.05$ $\varepsilon = 0.2$

N	O_{11}	O_{12}	O_{21}	O_{22}
80	-1.839	$1.720\ 10^{-1}$	-2.044	$1.304\ 10^{-1}$
160	-2.512	$1.142\ 10^{-1}$	-2.506	$8.245\ 10^{-2}$
320	-3.133	$7.351\ 10^{-2}$	-2.901	$5.022\ 10^{-2}$
640	-3.670	$4.621\ 10^{-2}$	-3.206	$2.961\ 10^{-2}$
1280	-4.107	$2.863\ 10^{-2}$	-3.414	$1.699\ 10^{-2}$
2560	-4.434	$1.763\ 10^{-2}$	-3.524	$9.561\ 10^{-3}$

$\lambda = 0.1$ $\varepsilon = 0$

N	O_{11}	O_{12}	O_{21}	O_{22}
80	-1.475	$1.417\ 10^{-1}$	-1.767	$9.410\ 10^{-2}$
160	-1.928	$8.144\ 10^{-2}$	-2.044	$4.536\ 10^{-2}$
320	-2.279	$4.036\ 10^{-2}$	-2.213	$1.467\ 10^{-2}$
640	-2.500	$1.442\ 10^{-2}$	-2.255	$-2.797\ 10^{-3}$
1280	-2.573	$-4.912\ 10^{-4}$	-2.163	$-1.127\ 10^{-2}$
2560	-2.491	$-7.924\ 10^{-3}$	-1.942	$-1.410\ 10^{-2}$

$\lambda = 0{,}1$ $\varepsilon = 0.1$

N	O_{11}	O_{12}	O_{21}	O_{22}
80	-1.435	$1.543\ 10^{-1}$	-1.720	$1.070\ 10^{-1}$
160	-1.888	$9.716\ 10^{-2}$	-1.993	$6.074\ 10^{-2}$
320	-2.262	$5.828\ 10^{-2}$	-2.177	$3.139\ 10^{-2}$
640	-2.540	$3.329\ 10^{-2}$	-2.260	$1.406\ 10^{-2}$
1280	-2.716	$1.806\ 10^{-2}$	-2.242	$4.619\ 10^{-3}$
2560	-2.794	$9.244\ 10^{-3}$	-2.132	$-1.833\ 10^{-5}$

$\lambda = 0.1$ $\varepsilon = 0.2$

N	O_{11}	O_{12}	O_{21}	O_{22}
80	-1.442	$1.642\ 10^{-1}$	-1.714	$1.176\ 10^{-1}$
160	-1.939	$1.087\ 10^{-1}$	-2.019	$7.252\ 10^{-2}$
320	-2.400	$7.059\ 10^{-2}$	-2.266	$4.338\ 10^{-2}$
640	-2.818	$4.527\ 10^{-2}$	-2.452	$2.537\ 10^{-2}$
1280	-3.191	$2.894\ 10^{-2}$	-2.578	$1.462\ 10^{-2}$
2560	-3.508	$1.857\ 10^{-2}$	-2.646	$8.377\ 10^{-3}$

$\lambda = 0.2$ $\varepsilon = 0$

N	O_{11}	O_{12}	O_{21}	O_{22}
80	-1.309	$1.297\ 10^{-1}$	-1.406	$6.790\ 10^{-2}$
160	-1.343	$7.242\ 10^{-2}$	-1.543	$2.438\ 10^{-2}$
320	-1.568	$3.434\ 10^{-2}$	-1.590	$-8.137\ 10^{-4}$
640	-1.698	$1.083\ 10^{-2}$	-1.542	$-1.343\ 10^{-2}$
1280	-1.727	$-2.338\ 10^{-3}$	-1.400	$-1.807\ 10^{-2}$
2560	-1.653	$-8.633\ 10^{-3}$	-1.75	$-1.809\ 10^{-2}$

$\lambda = 0.2$ $\varepsilon = 0.1$

N	O_{11}	O_{12}	O_{21}	O_{22}
80	-1.027	$1.485\ 10^{-1}$	-1.371	$8.938\ 10^{-2}$
160	-1.354	$9.454\ 10^{-2}$	-1.522	$4.788\ 10^{-2}$
320	-1.631	$5.827\ 10^{-2}$	-1.602	$2.298\ 10^{-2}$
640	-1.852	$3.498\ 10^{-2}$	-1.611	$9.096\ 10^{-3}$
1280	-2.019	$2.059\ 10^{-2}$	-1.553	$1.998\ 10^{-3}$
2560	-2.135	$1.198\ 10^{-2}$	-1.435	$-1.200\ 10^{-3}$

$\lambda = 0.2$ $\varepsilon = 0.2$

N	O_{11}	O_{12}	O_{21}	O_{22}
80	-1.083	$1.619\ 10^{-1}$	-1.396	$1.055\ 10^{-1}$
160	-1.484	$1.090\ 10^{-1}$	-1.601	$6.440\ 10^{-2}$
320	-1.883	$7.270\ 10^{-2}$	-1.769	$3.861\ 10^{-2}$
640	-2.284	$4.829\ 10^{-2}$	-1.903	$2.293\ 10^{-2}$
1280	-2.687	$3.215\ 10^{-2}$	-2.008	$1.362\ 10^{-2}$
2560	-3.073	$2.154\ 10^{-2}$	-2.081	$8.165\ 10^{-3}$

References

1 M.M. Elkind, R.S.I. 24, 129 /1953/

2 P.H. Rose, A. Galejs and L. Peck, N.I.M. 31, 262 /1964/

3 C.H. Johnson, J.P. Jidish and C.W. Snyder R.S.I. 28, 942 /1957/

4 V.A Romanov, A.N. Serbinov, Pribori i Technika Eksperiménta 5, 34 /1965/

5 J. Erő, E. Klopfer, P. Kostka, I. Kovács, I. Mérey, L. Vályi, L. Varga. Reports of the Central Research Institute for Physics. Budapest 13, 73 /1965/

6 Zworikin et al. Electron Optics and the Electron Microscope. /John Wiley and Sons, Ing., New York 1945/pp413 444.ff

7 L. Vályi, P. Gombos, J. Roósz Reports of the Central Research Institute for Physics. Budapest, 14, 259 /1966/

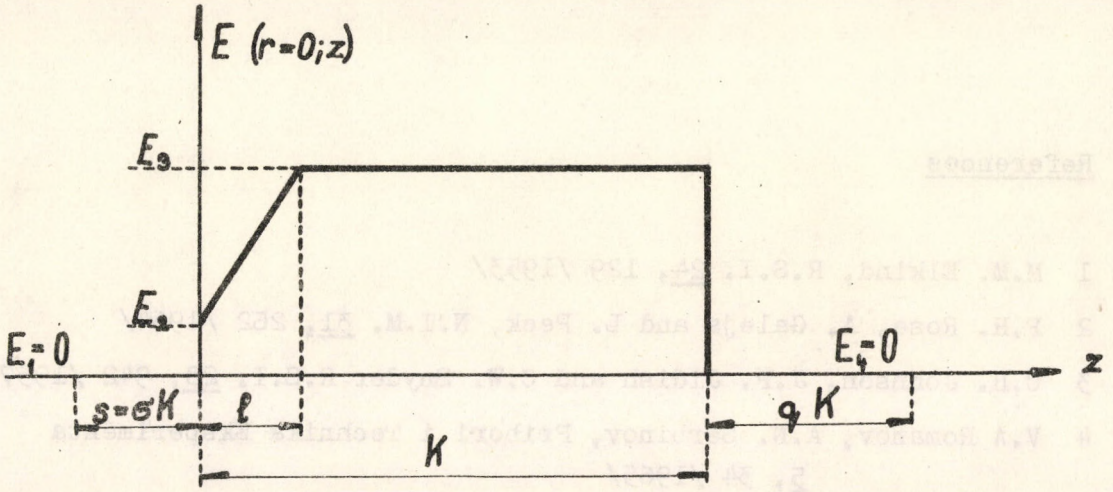

Fig. 1

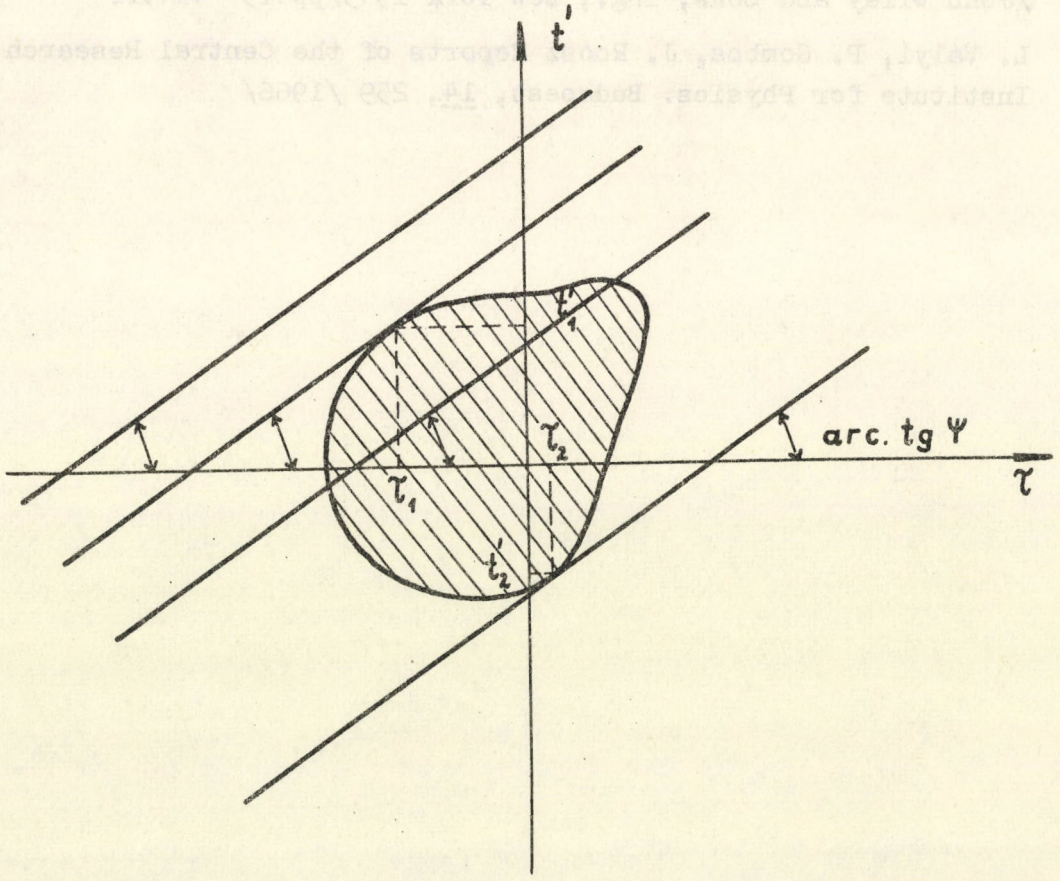

Fig. 2

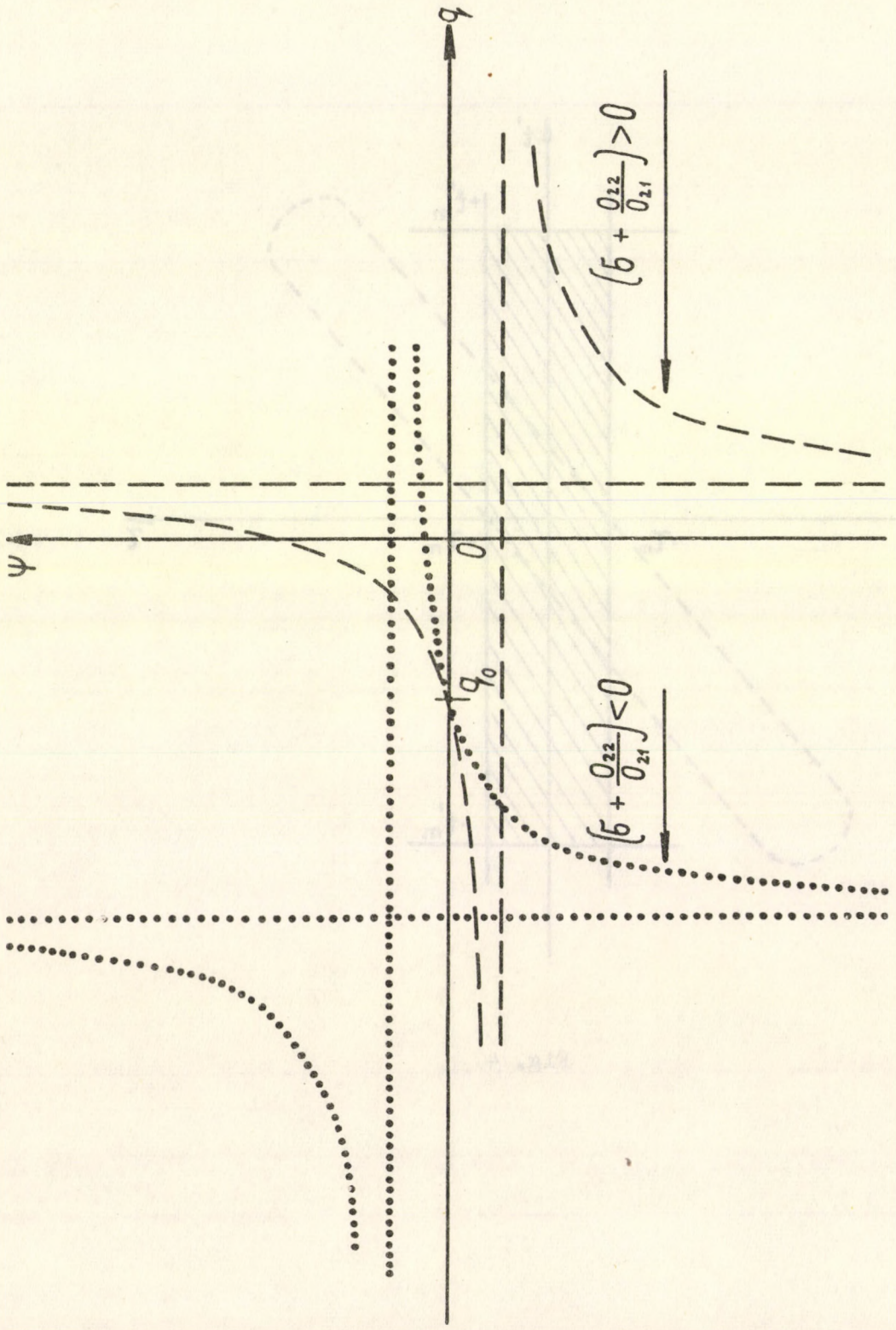
q
ψ
0
q_0
$\left(\sigma + \frac{\sigma_{12}}{\sigma_{21}}\right) > 0$
$\left(\sigma + \frac{\sigma_{22}}{\sigma_{21}}\right) < 0$

Fig. 3

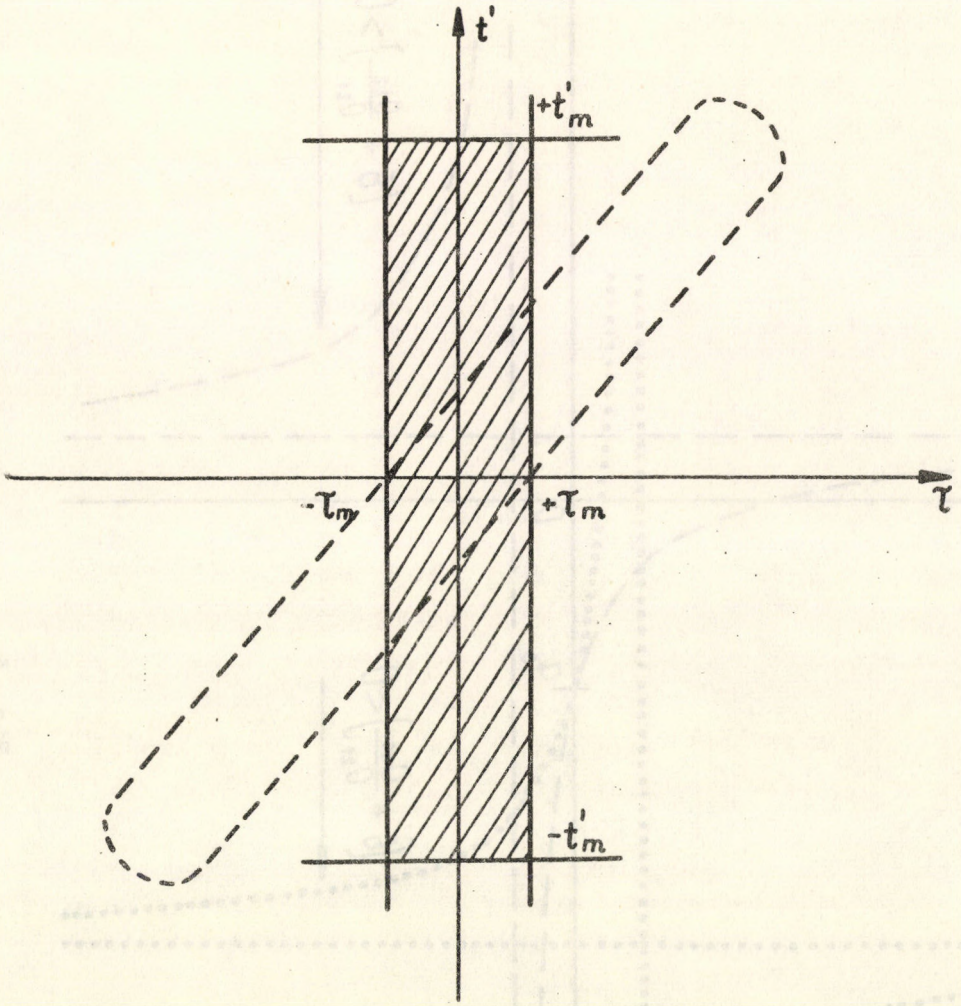

Fig. 4

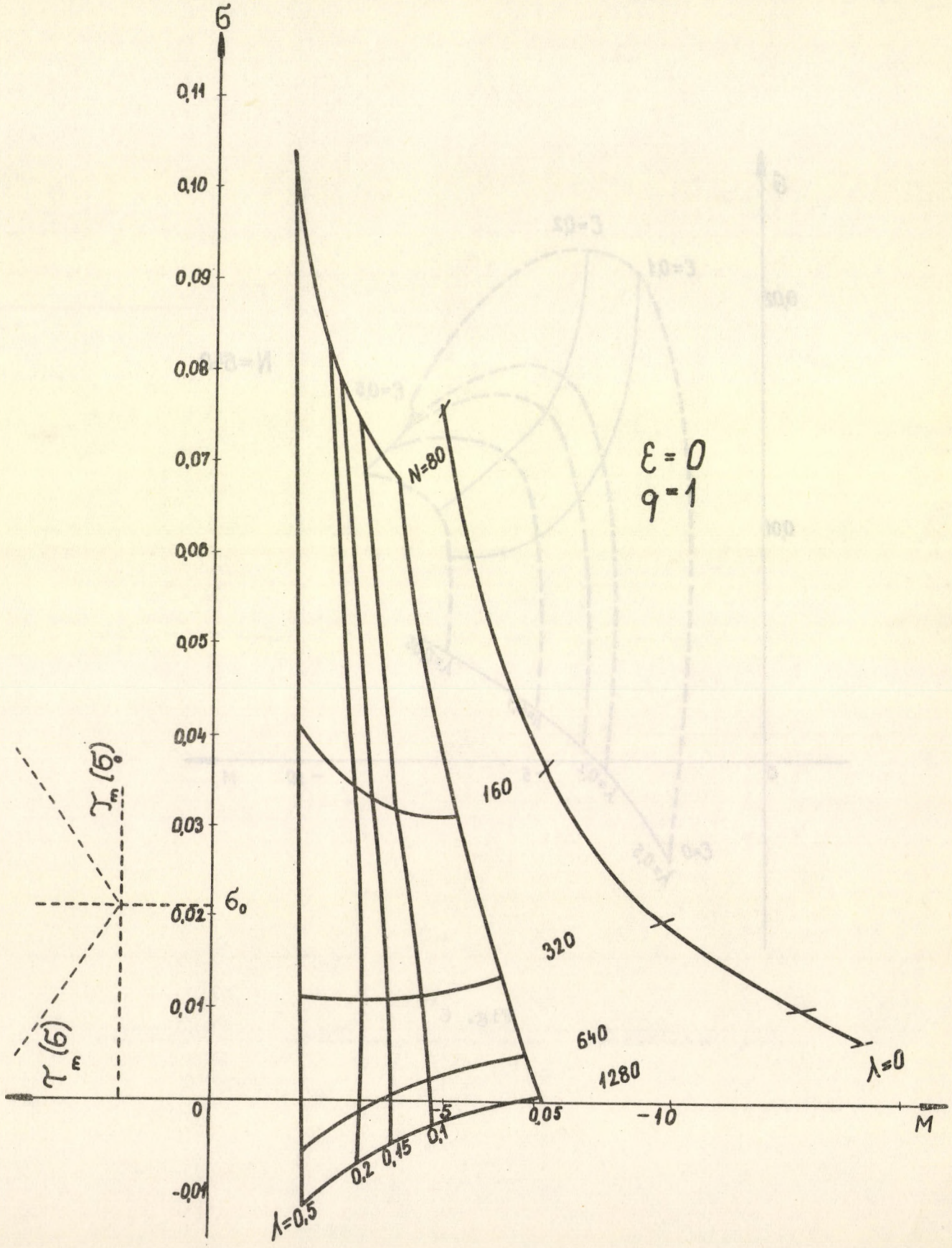
σ
0,11
0,10
0,09
0,08
0,07
0,06
0,05
0,04
0,03
0,02
0,01
0
-0,01
σ₀
τ_m(σ₀)
τ_ε(σ)
N=80
160
320
640
1280
λ=0
λ=0,5
0,2
0,15
0,1
0,05
-5
-10
M
ε=0
q=1

Fig. 5

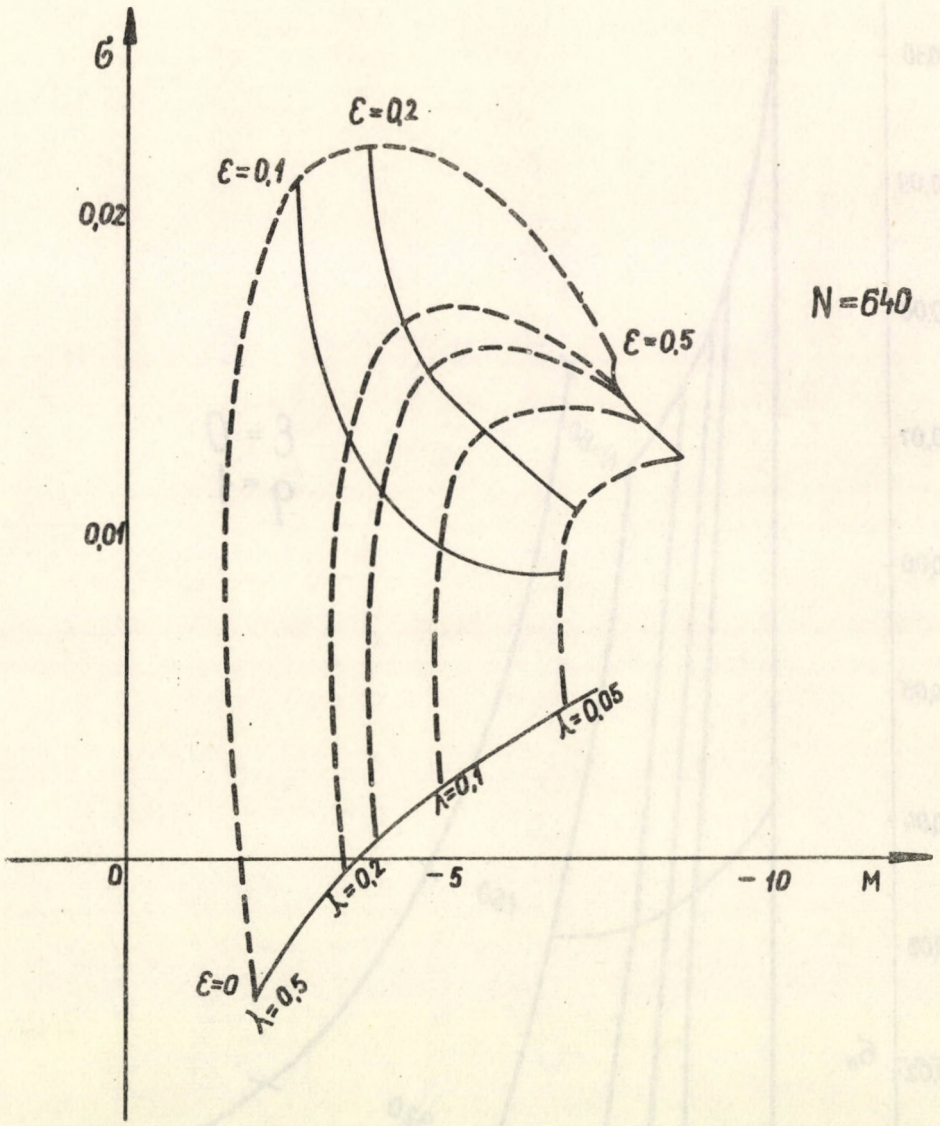

Fig. 6

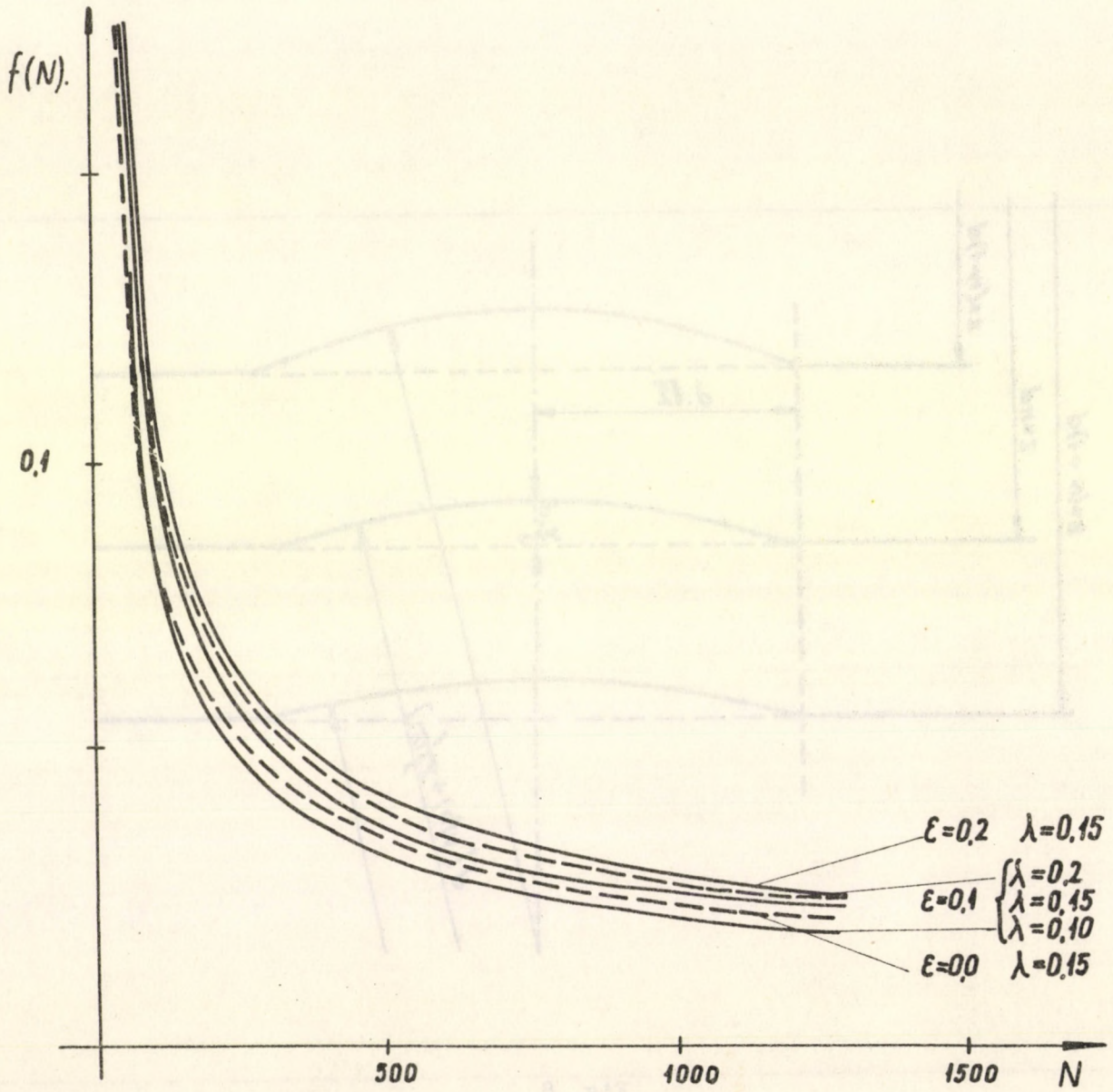

Fig. 7

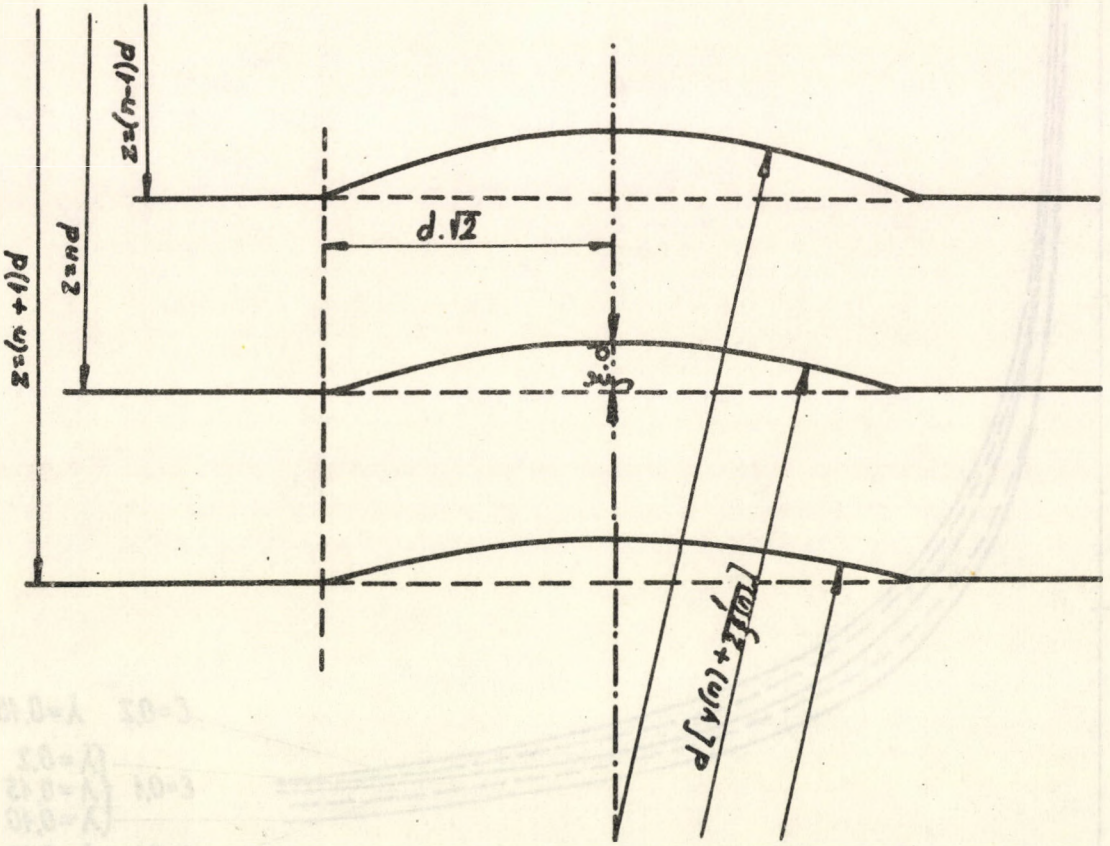

Fig. 8

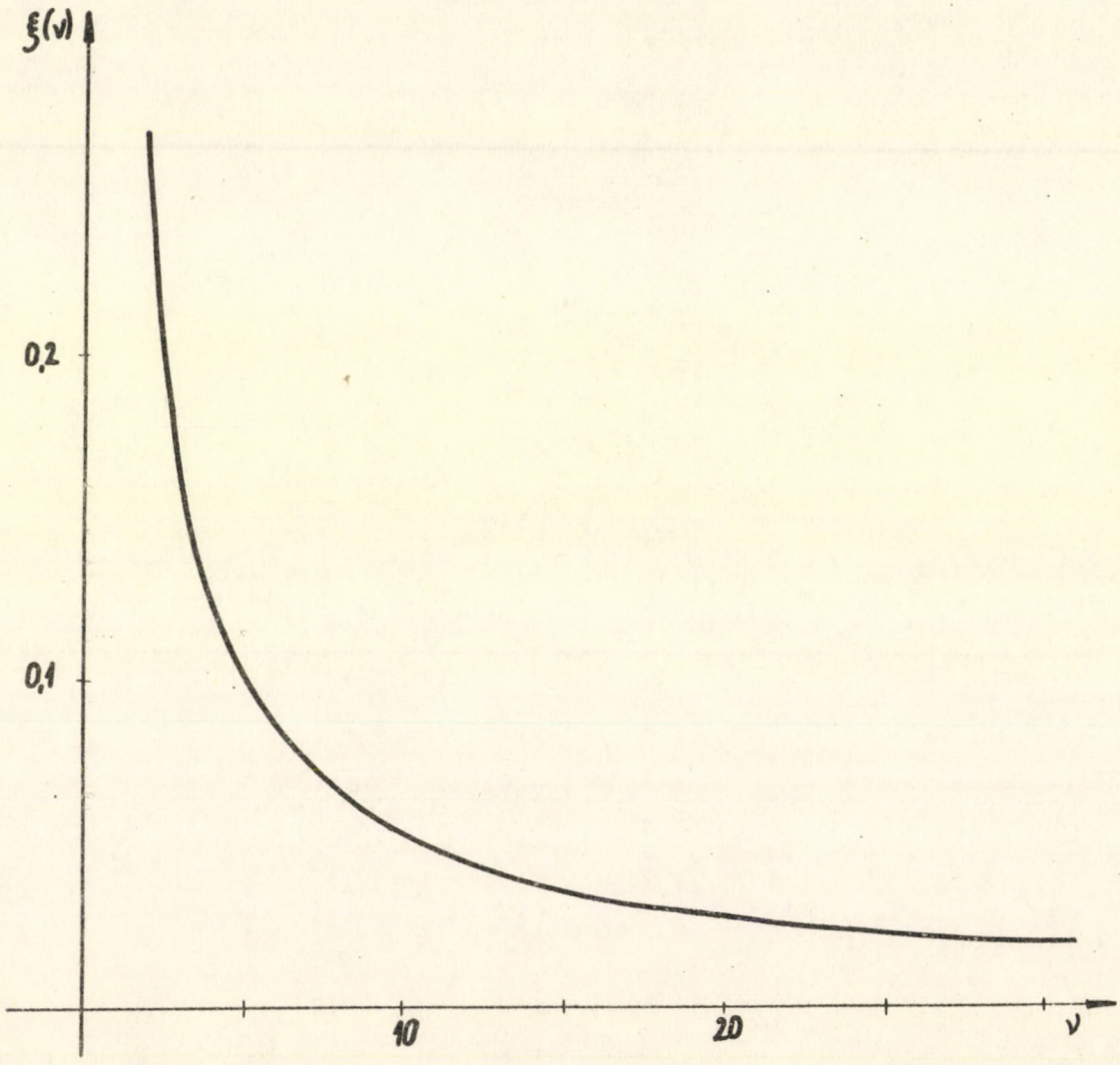

Fig. 9

Printed in the Central Research Institute for Physics, Budapest
Kiadja a KFKI Könyvtár- és Kiadói Osztály. Ov.:dr. Farkas Istvánné
Példányszám: 125 Munkaszám: 4191 Budapest, 1969. január 21.
Készült a KFKI házi sokszorositójában. Fv.: Gyenes Imre
Szakmai lektor: Hrehuss Gyula Nyelvi lektor: Kovács Jenőné

61.809